



Falkland Islands Fisheries Department

Falkland calamari Stock Assessment, Second Season 2016

Andreas Winter

October 2016

Index

Summary	3
Introduction.....	3
Methods.....	5
Stock assessment.....	7
Data.....	7
Group arrivals / depletion criteria.....	9
Depletion analyses	12
North.....	12
South.....	13
Escapement biomass.....	15
Immigration	16
Exploratory fishing	17
Bycatch	18
References.....	20
Appendix.....	23
Falkland calamari individual weights.....	23
Prior estimates and CV	24
Depletion model estimates and CV	26
Combined Bayesian models	27

Summary

- 1) The 2016 second season Falkland calamari fishery (X license) was open from July 29th, and closed by directed order on September 30th. Compensatory days for mechanical failures and bad weather resulted in 17 vessel-days taken after September 30th, with one vessel fishing as late as October 4th. Compensatory days did not increase the total season effort allocation.
- 2) 23,089 tonnes of calamari catch were reported in the X-license fishery; giving an average CPUE of 23.0 tonnes vessel-day⁻¹. Throughout the season 50.0% of calamari catch and 49.6% of fishing effort were taken north of 52° S; 49.9% of calamari catch and 50.2% of fishing effort were taken south of 52° S. One vessel took exploratory fishing north of the Loligo Box for 2 days; this was included in the north totals. Another vessel took exploratory fishing west of the Falkland Islands for 2 days; this was tabulated separately but included in the season catch / effort totals.
- 3) Sub-areas north and south of 52°S were depletion-modelled separately. In the north sub-area, three depletion periods / immigrations were inferred to have started on August 1st, August 5th, and – unusually late – October 1st. In the south sub-area, two depletion periods / immigrations were inferred to have started on July 29th and August 17th.
- 4) Approximately 21,799 tonnes of calamari (95% confidence interval: [14,351 to 49,467] tonnes) were estimated to have immigrated into the Loligo Box during second season 2016, of which 18,556 t north of 52° S and 3,243 t south of 52° S.
- 5) The escapement biomass estimate for calamari remaining in the Loligo Box at the end of second season 2016 was:
Maximum likelihood of 27,520 tonnes, with a 95% confidence interval of [18,757 to 51,411] tonnes.
The risk of calamari escapement biomass at the end of the season being less than 10,000 tonnes was estimated at < 0.01%.

Introduction

The second season of the 2016 Falkland calamari fishery (*Doryteuthis gahi* – Patagonian longfin squid – colloquially *Loligo*) opened on July 29th with 15 X-licensed vessels participating; the vessel that had conducted the pre-season survey took the flex option to start one day later. The season ended by directed closure on September 30th, making this the first complete second season under the new equalization schedule (Fisheries Committee, 2013). Two vessels experienced mechanical failures and were allocated 3-day extensions at the end of the season for time missed from the fishery, equivalent to the flex option. One vessel was replaced by a sister ship for 4 days. Another vessel was allocated one extra day for towing one of the damaged vessels to port. Ten vessels took a ‘bad weather’ day and ceased fishing on August 29th, a day of particularly strong wind from the north (Figure 1). Like flex days, bad weather days (up to 3) may be added back on the end of the season, notwithstanding any closure order. One vessel additionally took a ‘bad weather’ day on September 20th. With the combination of flex and weather allocations, 17 vessel-days were taken after the statutory end date of the season on September 30th. The last vessel finished fishing on October 4th.

Total reported Falkland calamari catch under second season X license was 23,089 tonnes (Table 1), corresponding to an average CPUE of $23089 / 1004 = 23.0$ tonnes vessel-day⁻¹. This average CPUE was the highest in a second season since 2012, and the third-highest in a second season of the past 10 years.

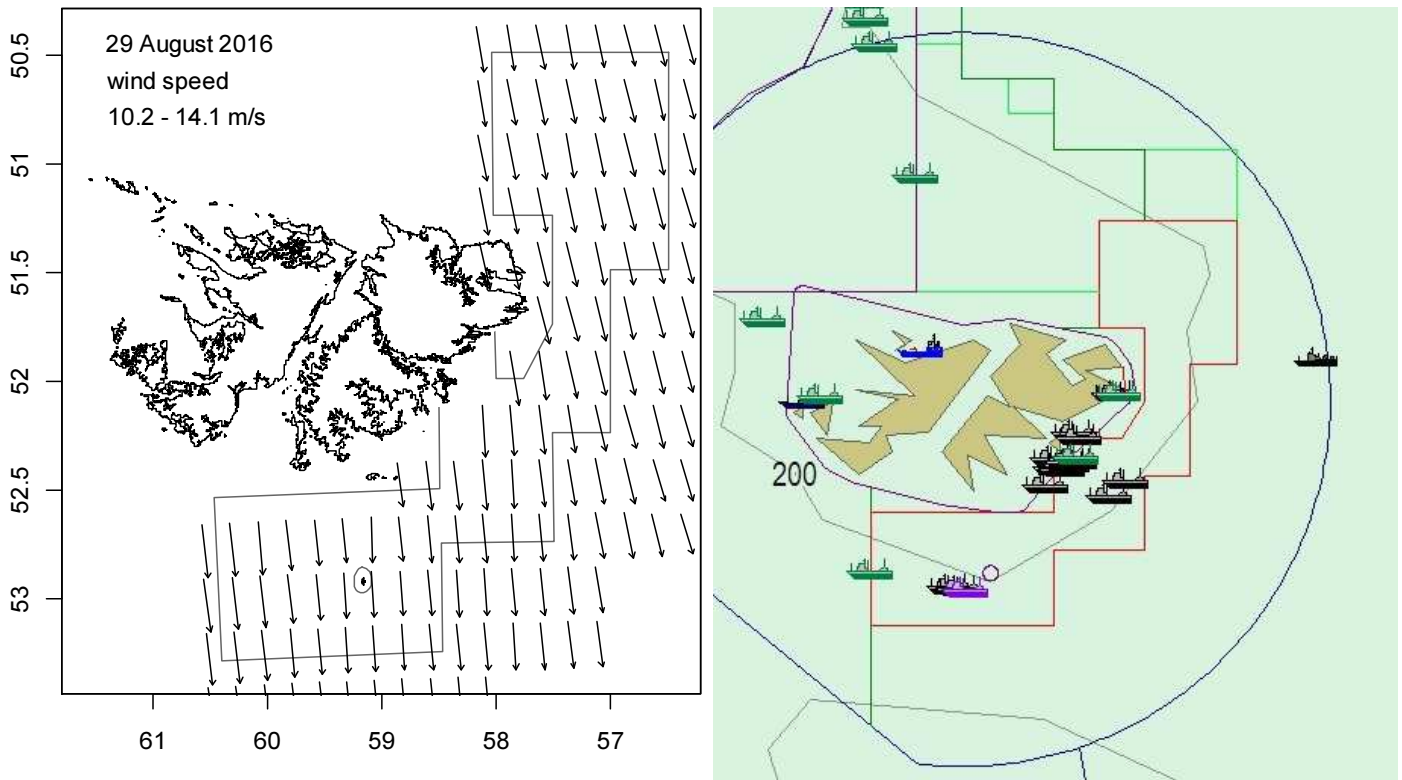


Figure 1. Left: wind speed vector plot at 0.25° resolution, from blended satellite observations (Zhang et al., 2006). Right: Fish Ops chart display. Both on August 29th when X-license fishing effort was reduced to 5 vessels because of weather conditions.

Table 1. Falkland calamari season comparisons since 2004. Days: total number of calendar days open to licensed calamari fishing including (since 1st season 2013) optional extension days; V-Days: aggregate number of licensed calamari fishing days reported by all vessels for the season. Entries in italics are seasons closed early by emergency order.

	Season 1			Season 2		
	Catch (t)	Days	V-Days	Catch (t)	Days	V-Days
2004	7,152	46	625	17,559	78	1271
2005	24,605	45	576	29,659	78	1210
2006	19,056	50	704	23,238	53	883
2007	17,229	50	680	24,171	63	1063
2008	24,752	51	780	26,996	78	1189
2009	12,764	50	773	17,836	59	923
2010	28,754	50	765	36,993	78	1169
2011	15,271	50	771	18,725	70	1099
2012	34,767	51	770	35,026	78	1095
2013	19,908	53	782	19,614	78	1195
2014	28,119	59	872	19,630	71	1099
2015	19,383*	57*	871*	10,190	42	665
2016	22,616	68	1020	23,089	68	1004

* Does not include C-license catch or effort after the C-license target for that season was switched from calamari to *Illex*.

As in previous seasons, the Falkland calamari stock assessment was conducted with depletion time-series models (Agnew et al., 1998; Roa-Ureta and Arkhipkin, 2007; Arkhipkin et al., 2008). Because calamari has an annual life cycle (Patterson, 1988), stock cannot be derived from a standing biomass carried over from prior years (Rosenberg et al., 1990; Pierce and Guerra, 1994). The depletion model instead calculates an estimate of population abundance over time by evaluating what levels of abundance and catchability must be extant to sustain the observed rate of catch. Depletion modelling is used both in-season and for the post-season summary, with the objective of maintaining an escapement biomass of 10,000 tonnes calamari at the end of each season as a conservation threshold (Agnew et al., 2002; Barton, 2002).

Methods

The depletion model formulated for the Falkland calamari stock is based on the equivalence:

$$C_{\text{day}} = q \times E_{\text{day}} \times N_{\text{day}} \times e^{-M/2} \quad (1)$$

where q is the catchability coefficient, M is the natural mortality rate (considered constant at 0.0133 day^{-1} ; Roa-Ureta and Arkhipkin, 2007), and C_{day} , E_{day} , N_{day} are catch (numbers of calamari), fishing effort (numbers of vessels), and abundance (numbers of calamari) per day. In its basic form (DeLury, 1947) the depletion model assumes a closed population in a fixed area for the duration of the assessment. However, the assumption of a closed population is imperfectly met in the Falkland Islands fishery, where stock analyses have often shown that calamari groups arrive in successive waves after the start of the season (Roa-Ureta, 2012; Winter and Arkhipkin, 2015). Arrivals of successive groups are inferred from discontinuities in the catch data. Fishing on a single, closed cohort would be expected to yield gradually decreasing CPUE, but gradually increasing average individual sizes, as the squid grow. When instead these data change suddenly, or in contrast to expectation, the immigration of a new group to the population is indicated (Winter and Arkhipkin 2015).

In the event of a new group arrival, the depletion calculation must be modified to account for this influx. This was done using a simultaneous algorithm (Roa-Ureta, 2012) that adds new arrivals on top of the stock previously present, and posits a common catchability coefficient for the entire depletion time-series. If two depletions are included in the same model (i.e., the stock present from the start plus a new group arrival), then:

$$C_{\text{day}} = q \times E_{\text{day}} \times (N1_{\text{day}} + (N2_{\text{day}} \times i2_{|_0}^1)) \times e^{-M/2} \quad (2)$$

where $i2$ is a dummy variable taking the values 0 or 1 if 'day' is before or after the start day of the second depletion. For more than two depletions, $N3_{\text{day}}$, $i3$, $N4_{\text{day}}$, $i4$, etc., would be included following the same pattern.

The Falkland calamari stock assessment was calculated in a Bayesian framework (Punt and Hilborn, 1997), whereby results of the season depletion model are conditioned by prior information on the stock; in this case the information from the pre-season survey. The season depletion likelihood function was calculated as the difference between actual catch numbers reported and catch numbers predicted from the model (equation 2), statistically corrected by a factor relating to the number of days of the depletion period (Roa-Ureta, 2012):

$$\left((nDays - 2) / 2 \right) \times \log \left(\sum_{days} \left(\log(\text{predicted } C_{\text{day}}) - \log(\text{actual } C_{\text{day}}) \right)^2 \right) \quad (3)$$

The survey prior likelihood function was calculated as the normal distribution of the difference between catchability (q) derived from the survey abundance estimate, and catchability derived from the season depletion model:

$$\frac{1}{\sqrt{2\pi \cdot SD_{q \text{ survey}}^2}} \times \exp \left(-\frac{(q_{\text{model}} - q_{\text{survey}})^2}{2 \cdot SD_{q \text{ survey}}^2} \right) \quad (4)$$

Catchability, rather than abundance N , was used for calculating the survey prior likelihood because catchability informs the entire season time series; whereas N from the survey only informs the first season depletion period – subsequent immigrations and depletions are independent of the abundance that was present during the survey.

Bayesian optimization of the depletion was calculated by jointly minimizing equations 3 and 4, using the Nelder-Mead algorithm in R programming package ‘optimx’ (Nash and Varadhan, 2011). Relative weights in the joint optimization were assigned to equations 3 and 4 as the converse of their coefficients of variation (CV), i.e., the CV of the prior became the weight of the depletion model and the CV of the depletion model became the weight of the prior. Calculations of the CVs are described in the Appendix. Because a complex model with multiple depletions may converge on a local rather than global minimum, the optimization was stabilized by running a feed-back loop that set the q and N parameter outputs of the Bayesian joint optimization back into the in-season only minimization (equation 3), re-calculated this minimization and the CV resulting from it, then re-calculated the Bayesian joint optimization, and continued this process until both the in-season minimization and the joint optimization remained unchanged.

With C_{day} , E_{day} and M being fixed parameters, the optimization of equation 2 using 3 and 4 produces estimates of q and N_1, N_2, \dots , etc. Numbers of calamari on the final day (or any other day) of a time series are then calculated as the numbers N of the depletion start days discounted for natural mortality during the intervening period, and subtracting cumulative catch also discounted for natural mortality (CNMD). Taking for example a two-depletion period:

$$N_{\text{final day}} = N1_{\text{start day 1}} \times e^{-M(\text{final day} - \text{start day 1})} + N2_{\text{start day 2}} \times e^{-M(\text{final day} - \text{start day 2})} - \text{CNMD}_{\text{final day}} \quad (5)$$

where

$$\begin{aligned} \text{CNMD}_{\text{day 1}} &= 0 \\ \text{CNMD}_{\text{day x}} &= \text{CNMD}_{\text{day x-1}} \times e^{-M} + C_{\text{day x-1}} \times e^{-M/2} \end{aligned} \quad (6)$$

$N_{\text{final day}}$ is then multiplied by the average individual weight of calamari on the final day to give biomass. Daily average individual weight is obtained from length / weight conversion of mantle lengths measured in-season by observers, and also derived from in-season commercial data as the proportion of product weight that vessels reported per market size category. Observer mantle lengths are scientifically accurate, but restricted to 1-2 vessels at any one time that may or may not be representative of the entire fleet, and not available every day.

Commercially proportioned mantle lengths are relatively less accurate, but cover the entire fishing fleet every day. Therefore, both sources of data are used (see Appendix).

Distributions of the likelihood estimates from joint optimization (i.e., measures of their statistical uncertainty) were computed using a Markov Chain Monte Carlo (MCMC) (Gamerman and Lopes, 2006), a method that is commonly employed for fisheries assessments (Magnusson et al., 2013). MCMC is an iterative process which generates random stepwise changes to the proposed outcome of a model (in this case, the q and N of calamari) and at each step, accepts or nullifies the change with a probability equivalent to how well the change fits the model parameters compared to the previous step. The resulting sequence of accepted or nullified changes (i.e., the ‘chain’) approximates the likelihood distribution of the model outcome. The MCMC of the depletion models were run for 200,000 iterations; the first 1000 iterations were discarded as burn-in sections (initial phases over which the algorithm stabilizes); and the chains were thinned by a factor equivalent to the maximum of either 5 or the inverse of the acceptance rate (e.g., if the acceptance rate was 12.5%, then every 8th (0.125^{-1}) iteration was retained) to reduce serial correlation. For each model three chains were run; one chain initiated with the parameter values obtained from the joint optimization of equations 3 and 4, one chain initiated with these parameters $\times 2$, and one chain initiated with these parameters $\times 1/4$. Convergence of the three chains was accepted if the variance among chains was less than 10% higher than the variance within chains (Brooks and Gelman, 1998). When convergence was satisfied the three chains were combined as one final set. Equations 5, 6, and the multiplication by average individual weight were applied to the CNMD and each iteration of N values in the final set, and the biomass outcomes from these calculations represent the distribution of the estimate. The peaks of the MCMC histograms were compared to the empirical optimizations of the N values.

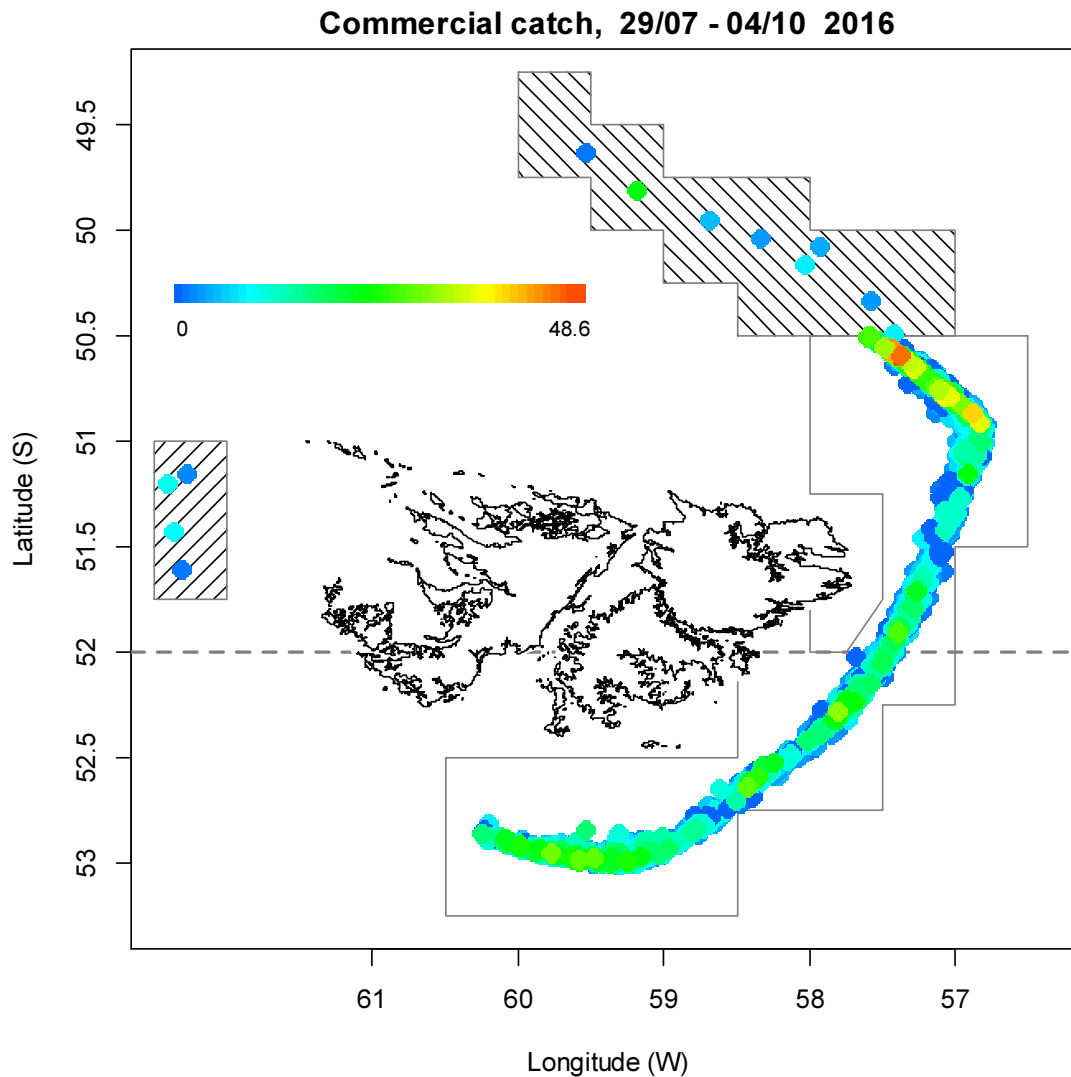
Total escapement biomass is defined as the aggregate biomass of calamari on the last day of the season for north and south sub-areas combined. Calamari sub-stocks emigrate from different spawning grounds and remain to an extent segregated (Arkhipkin and Middleton, 2002). However, it is not assumed that north and south biomasses are uncorrelated (Shaw et al., 2004), and therefore north and south likelihood distributions were added semi-randomly in proportion to the strength of their day-to-day correlation (see Winter, 2014, for the semi-randomization algorithm).

Stock assessment

Data

Total fishing effort in the 2nd season 2016 was distributed evenly with 50.0% of calamari catch and 49.6% of effort in the north sub-area (north of 52° S); 49.9% of catch and 50.2% of effort in the south sub-area. The north sub-area includes one vessel that took exploratory fishing north of the Loligo Box, but not the one vessel that took exploratory fishing out west (Figure 2, and see Exploratory fishing section), which accounted for 0.1% of calamari catch and 0.2% of effort. Preponderance of effort switched between north and south 13 times during the season (Figure 3).

Figure 2 [next page]. Spatial distribution of Falkland calamari 2nd-season commercial trawls, colour-scaled to catch weight (max. = 48.6 t per trawl). 3361 trawl catches were taken during the season. The ‘Loligo Box’ fishing zone, as well as the 52° S parallel delineating the boundary between north and south assessment sub-areas, are shown in grey. Additional grids shaded left-diagonally were open for exploratory calamari fishing to one vessel from September 4th to 5th. Grids shaded right-diagonally were open for exploratory calamari fishing to one vessel from September 30th to October 1st.



A total of 1004 vessel-days were fished during the season, with a median of 16 vessels per day (except for flex and weather extension days). Vessels reported daily catch totals to the FIFD and electronic logbook data that included trawl times, positions, and product weight by market size categories. Four FIFD observers were deployed on six vessels in the fishery for a total of 95 observer-days (Grimmer, 2016a; 2016b; Iriarte, 2016; Keningale, 2016). Throughout the 68 days of the season, 3 days had no observer covering, 39 days had 1 observer covering, 22 days had two observers covering, and 4 days had three observers covering. One vessel was also covered by the FIFD seabird observer for 17 days during the X-license fishery (Kuepfer, 2016). Observers sampled an average of 420 calamari daily, and reported their maturity stages, sex, and lengths to 0.5 cm. The length-weight relationship for converting both observer and commercially proportioned length data was taken from the pre-season survey (Winter et al., 2016):

$$\text{weight (kg)} = 0.128 \times \text{length (cm)}^{2.322} / 1000 \quad (7)$$

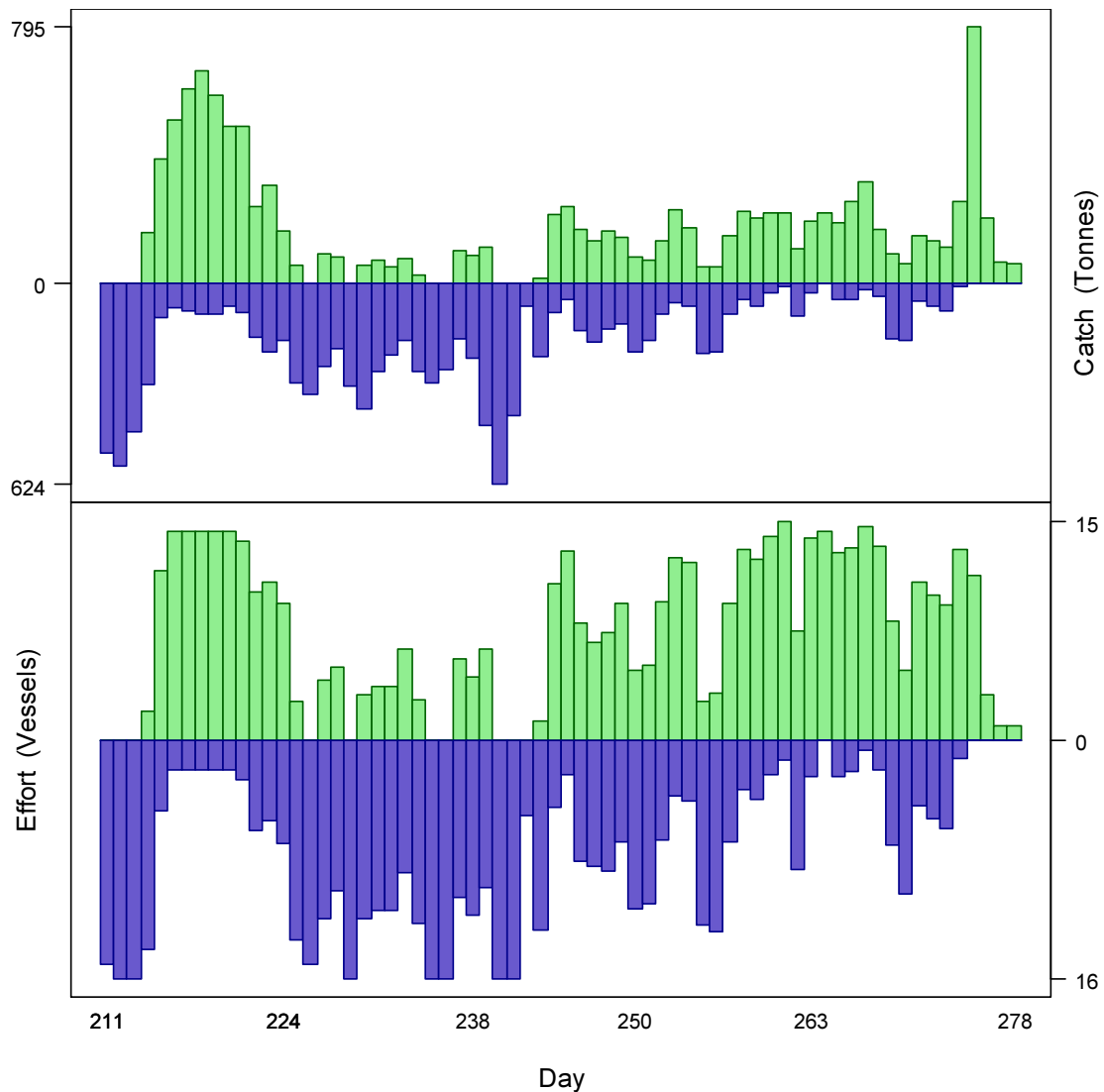


Figure 3. Daily total Falkland calamari catch and effort distribution by assessment sub-area north (green) and south (purple) of the 52° S parallel during 2nd season 2016. The season was open from July 29th (chronological day 211) to September 30th (chronological day 274), plus flex days until October 4th (day 278). As many as 15 vessels fished per day north of 52° S; as many as 16 vessels fished per day south of 52° S. As much as 795 tonnes calamari was caught per day north of 52° S; as much as 624 tonnes calamari was caught per day south of 52° S.

Group arrivals / depletion criteria

Start days of depletions - following arrivals of new calamari groups - were judged primarily with reference to daily changes in CPUE, with additional information from sex proportions, maturity, and average individual calamari sizes. CPUE was calculated as metric tonnes of calamari caught per vessel per day. Days were used rather than trawl hours as the basic unit of effort. Commercial vessels do not trawl standardized duration hours, but rather durations that best suit their daily processing requirements. An effort index of days is therefore more consistent.

Three days in the north and two days in the south were identified that represented the onset of separate immigrations / depletions in the season.

- The first depletion north was identified on day 214 (August 1st), three days after the start of the season and the date on which commercial fishing was first undertaken in the north (by 2 vessels). Average CPUE by these two vessels on day 214 was the highest in the north all season (77.6 t vessel⁻¹ day⁻¹) (Figure 4).
- The second depletion north was identified just four days later on day 218 (August 5th) with a CPUE increase over 3 days to the highest level (47.1 t vessel⁻¹ day⁻¹) until day 275 (Figure 4). On day 218 observer weight averages decreased to local minima (Figure 5B) and the proportion of females increased to the highest of the season up to that point (Figure 5C).
- The third depletion north was identified on day 275 (October 1st) with a very strong CPUE increase to the highest level since day 214 (72.3 t vessel⁻¹ day⁻¹) (Figure 4). Concurrently the proportion of females dropped sharply (Figure 5C) and weight averages decreased two days later (Figure 5A & B).
- The first depletion south was identified on day 211 (July 29th – start of the commercial season) with 15 vessels starting the fishery in the south (Figure 3) and moderately high CPUE that sustained for two days (35.0 and 35.5 t vessel⁻¹ day⁻¹) (Figure 4).
- The second depletion south was identified on day 230 (August 17th). CPUE increased to 32.7 t vessel⁻¹ day⁻¹ following six days of decrease (Figure 4), and one day after local minima in weight averages (Figure 5A & B).

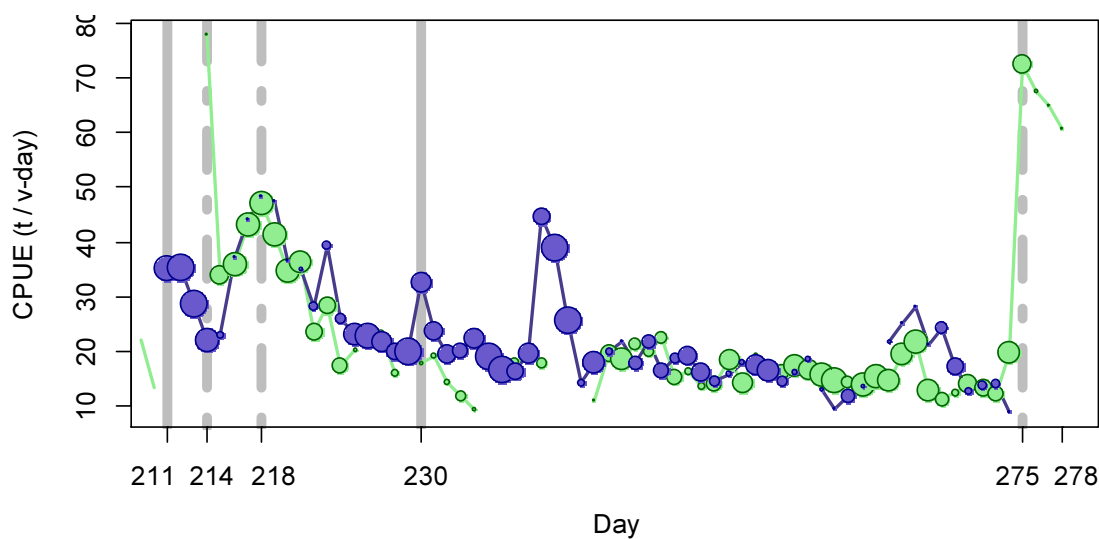
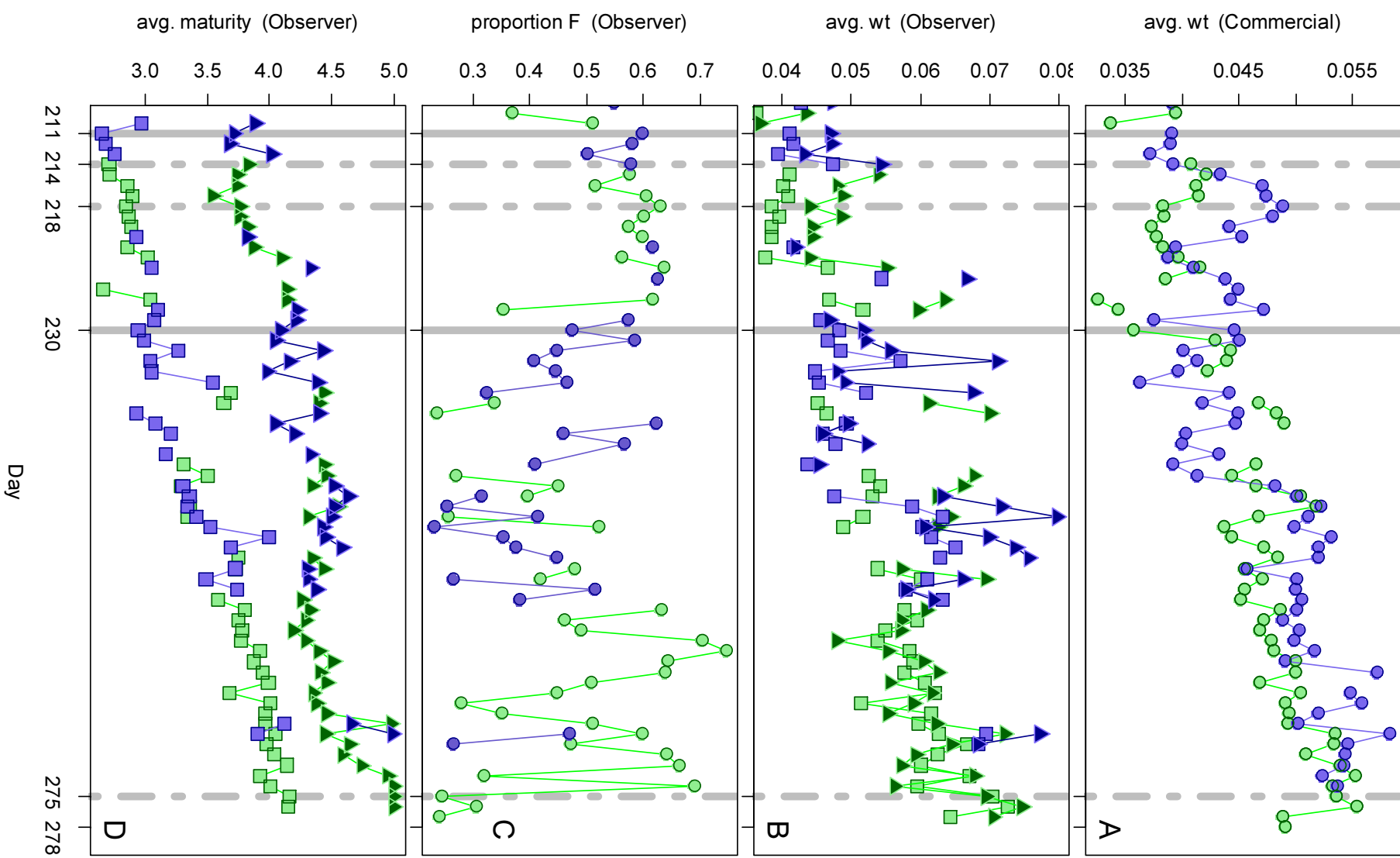


Figure 4. CPUE in metric tonnes per vessel per day, by assessment sub-area north (green) and south (purple) of 52° S latitude. Circle sizes are proportioned to numbers of vessels fishing. Data from consecutive days are joined by line segments. Broken grey bars indicate the starts of in-season depletions north. Solid grey bars indicate the starts of in-season depletions south.

Figure 5 [next page]. A: Average individual calamari weights (kg) per day from commercial size categories. B: Average individual calamari weights (kg) by sex per day from observer sampling. C: Proportions of female calamari per day from observer sampling. D: avg. maturity value by sex per day from observer sampling. In all graphs – Males: triangles, females: squares, unsexed: circles. North sub-area: green, south sub-area: purple. Data from consecutive days are joined by line segments. Broken grey bars indicate the starts of in-season depletions north. Solid grey bars indicate the starts of in-season depletions south.



Depletion analyses North

In the north sub-area, Bayesian optimization on catchability (q) resulted in a posterior (max. likelihood $q_{\text{Bayesian}} = 2.916 \times 10^{-3}$; Figure 6, left, and Equation A9-N) that was closer to the pre-season prior (prior $q_{\text{N}} = 4.109 \times 10^{-3}$; Figure 6, left, and Equation A4-N) than to the in-season depletion (depletion $q_{\text{N}} = 8.803 \times 10^{-4}$; Figure 6, left, and A6-N). Respective weights in the Bayesian optimization (converse of the CVs) were 0.404 for the in-season depletion (A5-N) and 0.366 for the prior (A8-N).

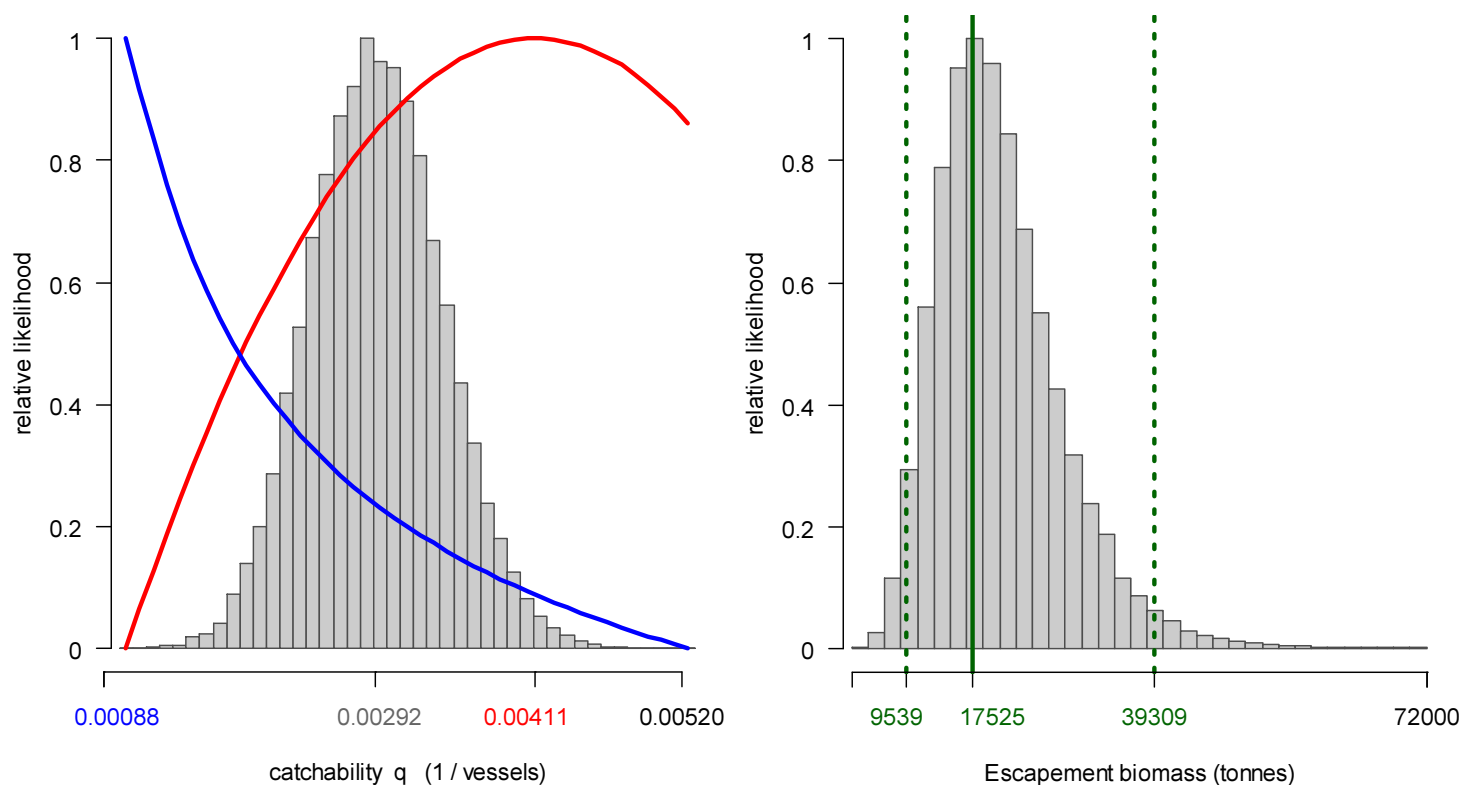


Figure 6. North sub-area. Left: Likelihood distributions for calamari catchability. Red line: prior model (pre-season survey data), blue line: in-season depletion model, grey bars: combined Bayesian model posterior. Right: Likelihood distribution (grey bars) of escapement biomass, from Bayesian posterior and average individual calamari weight at the end of the season. Green lines: maximum likelihood and 95% confidence interval. Note the correspondence to Figure 7.

The MCMC distribution of the Bayesian posterior multiplied by the GAM fit of average individual calamari weight (Figure A1-north) gave the likelihood distribution of calamari biomass on day 278 (October 4th) shown in Figure 6-right, with maximum likelihood and 95% confidence interval of:

$$B_{\text{N day 278}} = 17,525 \text{ t} \sim 95\% \text{ CI } [9,539 - 39,309] \text{ t} \quad (8)$$

At its highest point (last depletion start: day 275 – October 1st), estimated calamari biomass north was 19,066 t \sim 95% CI [10,867 – 41,431] t (Figure 7).

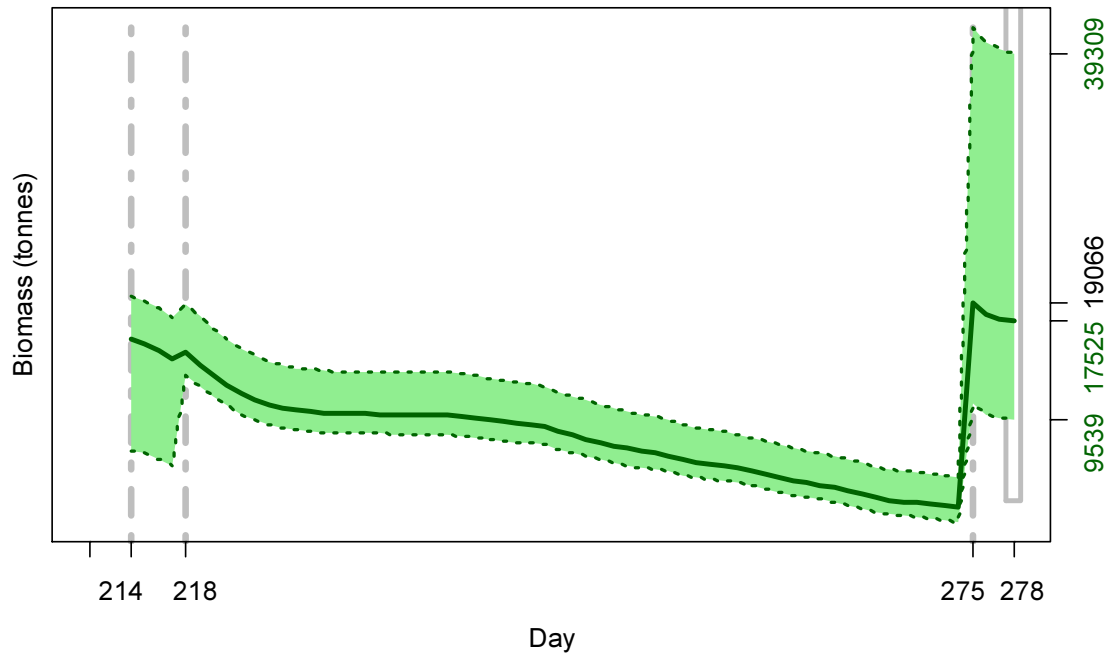


Figure 7. North sub-area. Calamari biomass time series estimated from Bayesian posterior of the depletion model \pm 95% confidence intervals. Broken grey bars indicate the start of in-season depletions north; days 214, 218 and 275. Note that the biomass ‘footprint’ on day 278 (October 4th) corresponds to the right-side plot of Figure 6.

South

In the south sub-area, Bayesian optimization on catchability (q) resulted in a posterior (maximum likelihood Bayesian $q_S = 1.120 \times 10^{-3}$; Figure 8, left, and Equation A9-N) that was intermediate between the pre-season prior (prior $q_S = 1.161 \times 10^{-3}$; Figure 8, left, and Equation A4-N) and the in-season depletion depletion $q_S = 0.649 \times 10^{-3}$ (Figure 8, left, and A6-S). Bayesian optimization was weighted 0.455 for in-season depletion (A5-S) vs. 0.360 for the prior (A8-S).

The MCMC distribution of the Bayesian posterior multiplied by the GAM fit of average individual calamari weight (Figure A1-south) gave the likelihood distribution of calamari biomass on day 278 (October 4th) shown in Figure 8-right, with maximum likelihood and 95% confidence interval of:

$$B_{S \text{ day } 278} = 10,180 \text{ t} \sim 95\% \text{ CI } [7,715 - 15,499] \text{ t} \quad (9)$$

At its highest point (on the first day of the season, day 211; July 29th), estimated calamari biomass south was 30,888 t \sim 95% CI [23,833 – 41,448] t (Figure 9).

Figure 8 [next page]. South sub-area. Left: Likelihood distributions for calamari catchability. Red line: prior model (pre-season survey data), blue line: in-season depletion model, grey bars: combined Bayesian model posterior. Right: Likelihood distribution (grey bars) of escapement biomass, from Bayesian posterior and average individual calamari weight at the end of the season. Blue lines: maximum likelihood and 95% confidence interval. Note correspondence to Figure 9.

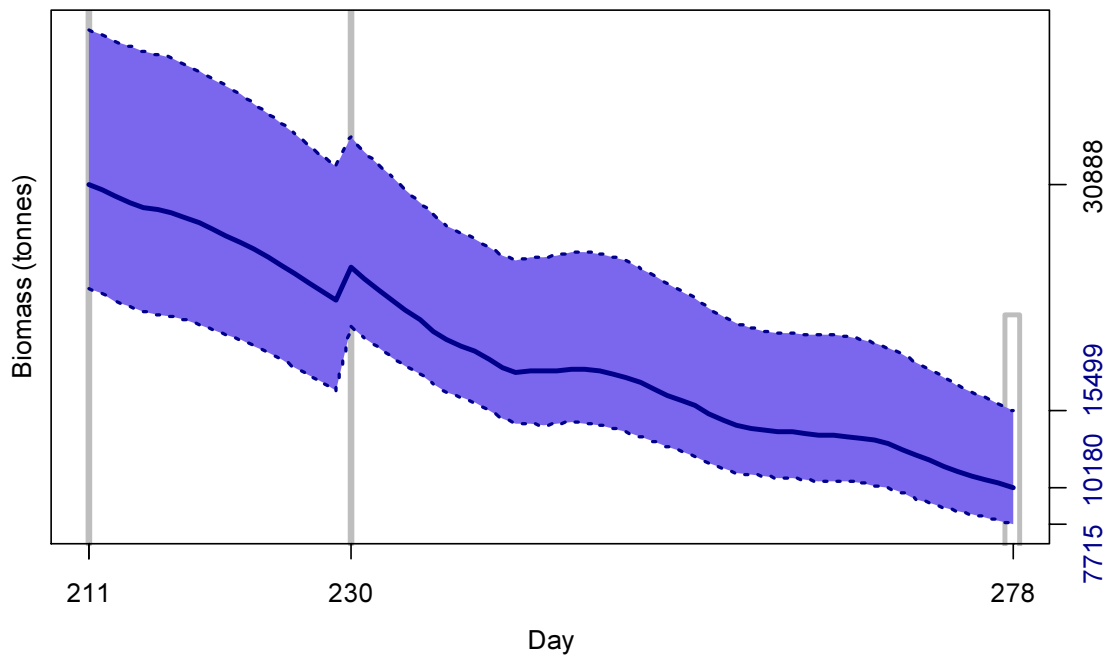
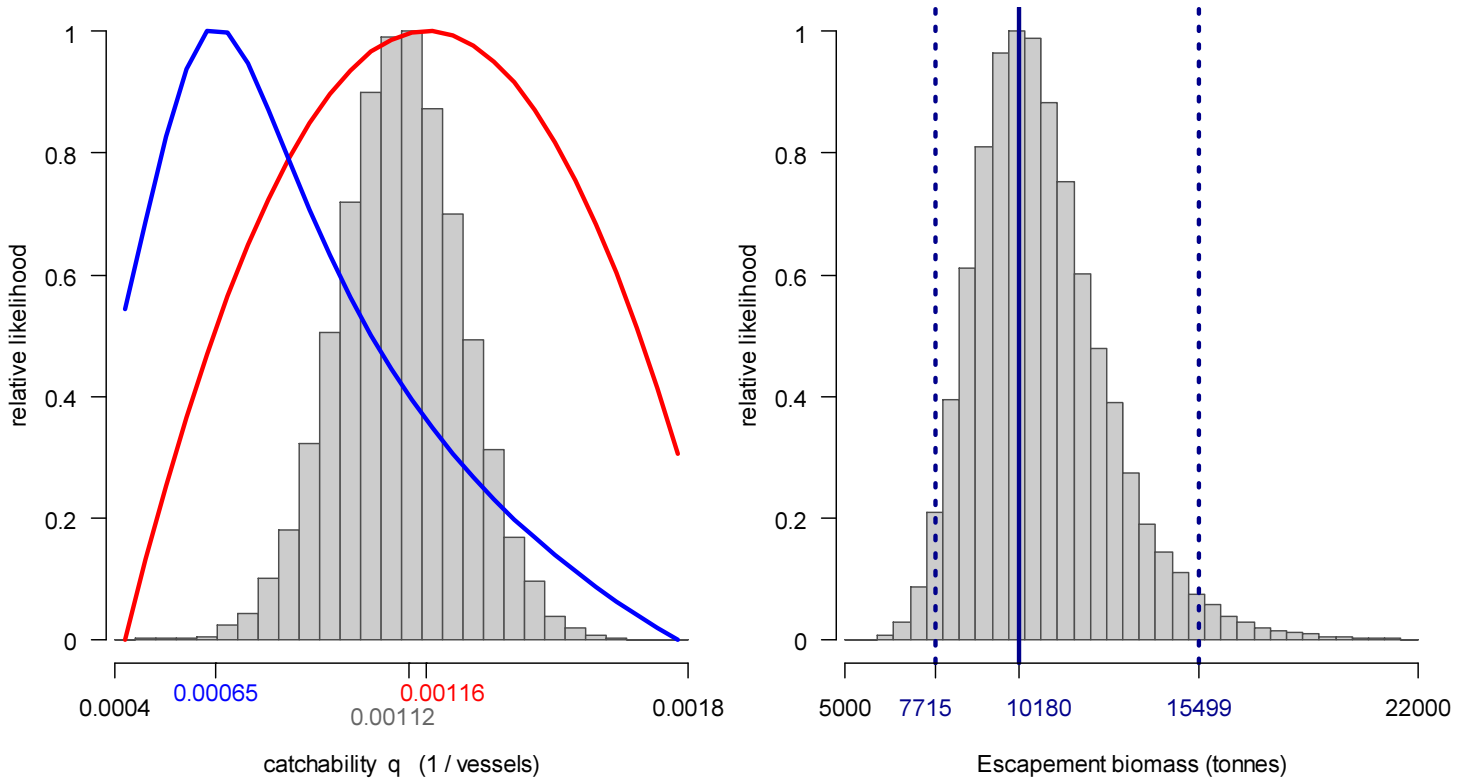


Figure 9. South sub-area. Calamari biomass time series estimated from Bayesian posterior of the depletion model \pm 95% confidence intervals. Gray bars indicate the start of in-season depletions south; days 211 and 230. Note that the biomass ‘footprint’ on day 278 (October 4th) corresponds to the right-side plot of Figure 8.

Escapement biomass

Total escapement biomass was defined as the aggregate biomass of Falkland calamari at the end of day 278 (October 4th) for north and south sub-areas combined (equations 8 and 9). Depletion models are calculated on the inference that all fishing and natural mortality are gathered at mid-day, thus a half day of mortality ($e^{-M/2}$) was added to correspond to the closure of the fishery at 23:59 (mid-night) on October 4th for the final remaining vessel: equation 10. Semi-randomized addition of the north and south biomass estimates gave the aggregate likelihood distribution of total escapement biomass shown in Figure 10.

$$\begin{aligned}
 B_{\text{Total day 278}} &= (B_{\text{N day 278}} + B_{\text{S day 278}}) \times e^{-M/2} \\
 &= 27,705 \text{ t} \times 0.9934 \\
 &= 27,520 \text{ t} \sim 95\% \text{ CI } [18,757 - 51,411] \text{ t}
 \end{aligned}
 \tag{10}$$

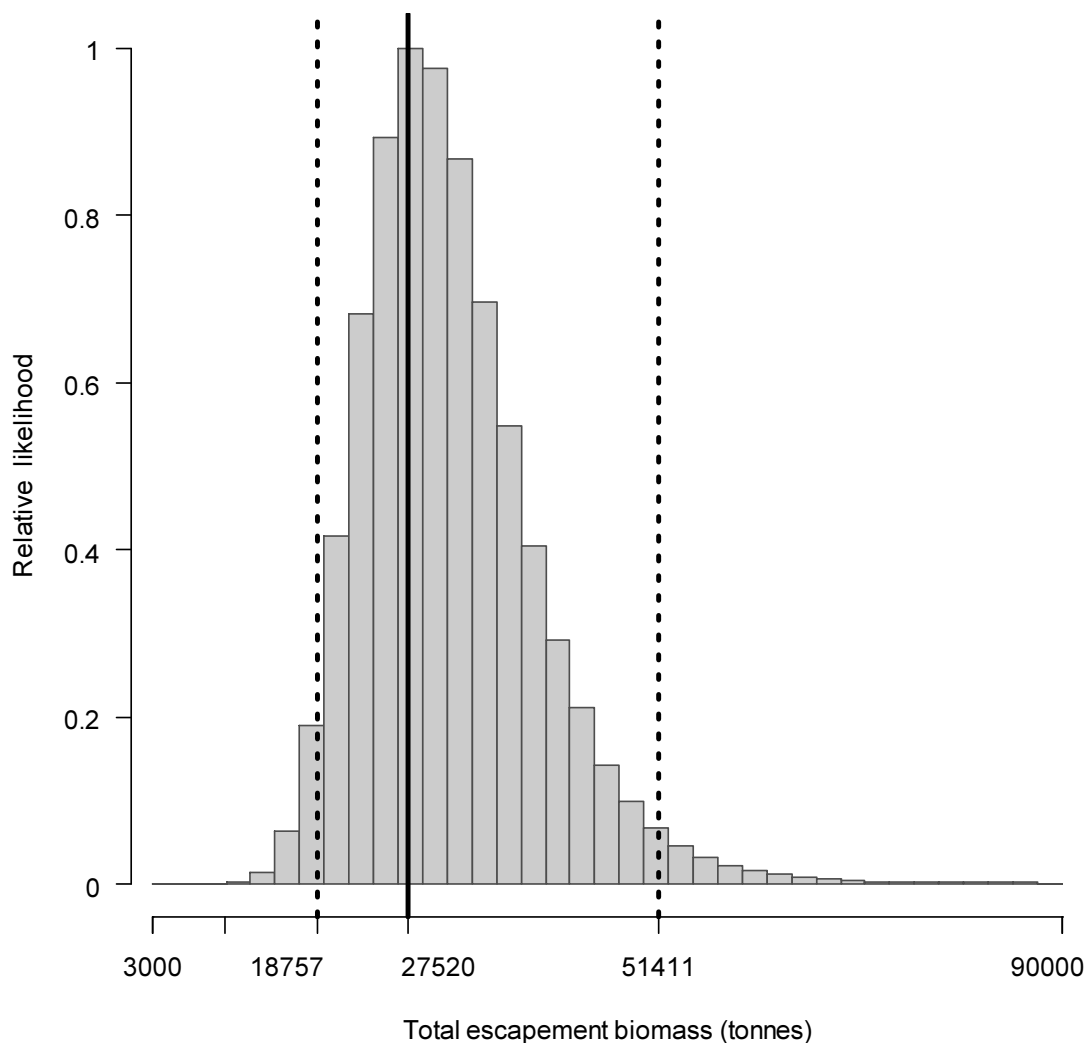


Figure 10. Likelihood distribution with 95% confidence intervals of total Falkland calamari escapement biomass corresponding to the season end (October 4th).

The risk of the fishery in the current season, defined as the proportion of the total escapement biomass distribution below the conservation limit of 10,000 tonnes (Agnew et al., 2002; Barton, 2002), was calculated as < 0.01%.

The escapement biomass total of 27,520 tonnes was the highest in a 2nd season since 2012 (which was also the most recent 2nd season to have achieved higher catches than the current season, Table 1). That fishery risk in the current season was not absolute zero despite an escapement biomass nearly 3× the escapement threshold attests to the high variability imposed by the very late (October 1st) immigration in the north (Figure 7). This late immigration also produced the unusual situation that season-end biomass in the north sub-area (17,525 t; above) was estimated higher than the pre-season biomass (15,844 t; Winter et al., 2016).

Immigration

Falkland calamari immigration during the season was inferred on each day by how many more calamari were estimated present than the day before, minus the number caught and the number expected to have died naturally:

$$\text{Immigration } N_{\text{day } i} = N_{\text{day } i} - (N_{\text{day } i-1} - C_{\text{day } i-1} - M_{\text{day } i-1})$$

where $N_{\text{day } i-1}$ are optimized in the depletion models, $C_{\text{day } i-1}$ calculated as in equation 2, and $M_{\text{day } i-1}$ is:

$$M_{\text{day } i-1} = (N_{\text{day } i-1} - C_{\text{day } i-1}) \times (1 - e^{-M})$$

Immigration biomass per day was then calculated as the immigration number per day multiplied by predicted average individual weight from the GAM:

$$\text{Immigration } B_{\text{day } i} = \text{Immigration } N_{\text{day } i} \times \text{GAM } W_{\text{day } i}$$

All numbers N are themselves derived from the daily average individual weights, so the estimation factors in that those calamari immigrating on a day would likely be smaller than average. Confidence intervals of the immigration estimates were calculated by applying the above algorithms to the MCMC iterations of the depletion models. Resulting total biomasses of calamari immigration north and south, up to season end (day 278), were:

$$\text{Immigration } B_{N \text{ day } 214-278} = 18,556 \text{ t} \sim 95\% \text{ CI } [12,283 - 43,885] \text{ t} \quad \text{(11-N)}$$

$$\text{Immigration } B_{S \text{ day } 211-278} = 3,243 \text{ t} \sim 95\% \text{ CI } [407 - 8,392] \text{ t} \quad \text{(11-S)}$$

Total immigration with semi-randomized addition of the confidence intervals was:

$$\text{Immigration } B_{\text{Total } 211-278} = 21,799 \text{ t} \sim 95\% \text{ CI } [14,351 - 49,467] \text{ t} \quad \text{(11-T)}$$

In the north sub-area, the in-season peaks on days 218 and 275 accounted for approximately 6.9% and 85.4% of in-season immigration (start day 214 was de facto not an in-season immigration), consistent with the variation in the time series biomass shown on Figure 7. In the south sub-area, the in-season peak on day 230 accounted for approximately 71.2% of in-season immigration (cf. Figure 9).

Exploratory fishing

Two X-licensed vessels were permitted to conduct exploratory calamari fishing during the season in grids outside the Loligo Box. One vessel was permitted to fish in grids XKAP, XKAN, XKAN, XJAP, XJAN, XJAM, XJAL, XHAM, XHAL, XHAK, XGAK, XGAJ and XFAJ, adjacent north-north-west of the Loligo Box (Figure 2), initially for two days on September 4th and 5th. This permit was subject to the conditions of no more than two trawls per grid, at least 1 mile apart, and the vessel carried a FIFD observer. A second vessel was permitted to fish in grids XNAD, XPAD and XQAD, west of the Falkland Islands (Figure 2), initially for two days on September 30th and October 1st, and subject to the same conditions.

The vessel fishing north took 4 trawls on September 4th, traversing grids XJAN, XJAM, XHAL, XHAK, XGAK and XGAJ, and 3 trawls on September 5th, traversing grids XKAP, XKAN, XJAN, XJAM and XHAM. This vessel was authorized to extend exploratory fishing for a further two days thereafter but elected not to. Following procedures used for exploratory fishing assessment in the previous two 2nd seasons (Winter, 2014; 2015), the exploratory catches on September 4th and 5th were compared to the average of vessels fishing in the top three ‘rows’ of the Loligo Box (between 50.5° S and 51.25° S) on the same days plus one day before and after. These data are shown in Table 2. To avoid identifying the exploratory vessel’s catches outright, data are standardized to “1” as the maximum average calamari catch rate. On its first day north of the Loligo Box the exploratory vessel achieved the highest calamari catch rates of this block of comparisons, but by the next day catch rates north of the Loligo Box had dropped below the average of calamari catch rates inside the north Loligo Box. Catch rates of rock cod (*Patagonotothen ramsayi*) were not higher north of the Loligo Box; catch rates of other bycatch were higher north of the Loligo Box but not by important margins (Table 2). These outcomes are typical for exploratory calamari fishing in the past few years (Winter, 2014; 2015).

The vessel fishing west of the Falkland Islands took 2 trawls on September 30th, traversing grids XPAD and XQAD, and 2 trawls on October 1st, in grid XNAD. Calamari in the west cannot be considered an extension of the aggregations either north or south in the Loligo Box, but a comparison of proportional catch rates and average individual calamari weights is shown in Table 3. Catch rates and average individual weights by the one vessel fishing west were similar on those days to the Loligo Box before the last immigration in the north on October 1st.

Table 2. Proportional (max. = 1) catch rates of calamari (LOL), rock cod (PAR) and other bycatch of the X-licensed vessel permitted to fish north of the Loligo Box, compared to vessels (N = number per day) that fished by regular license statute in the northern part of the Loligo Box over the same range of days.

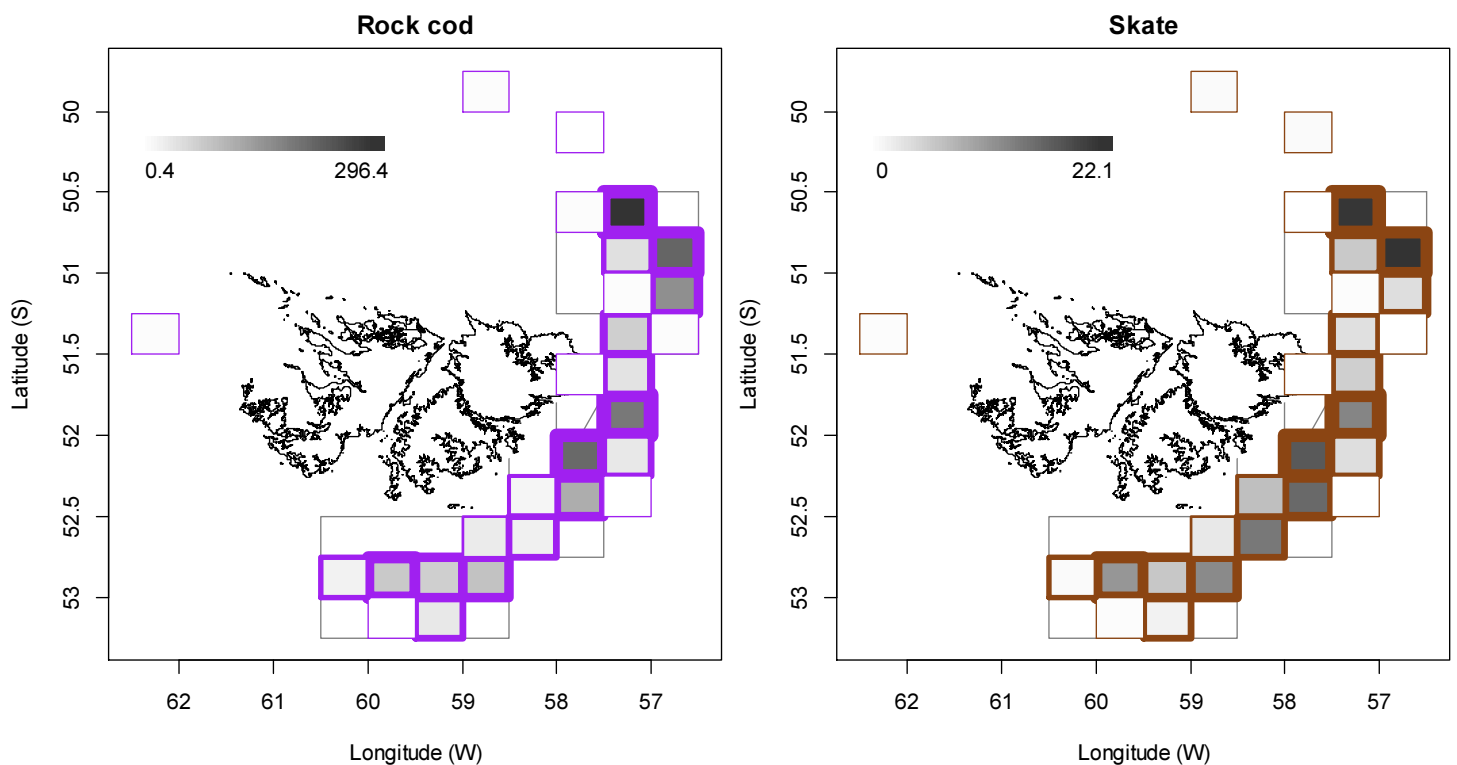
Date	Vessel North of Box				Vessels inside North Box			
	N	LOL	PAR	Other Bycatch	N	LOL	PAR	Other Bycatch
03/09	0	-	-	-	2	0.564	0.059	0.027
04/09	1	1.000	0.054	0.142	3	0.651	0.047	0.040
05/09	1	0.257	0.029	0.040	6	0.434	0.060	0.024
06/09	0	-	-	-	3	0.529	0.129	0.006
Avg.		0.629	0.042	0.091		0.519	0.072	0.024

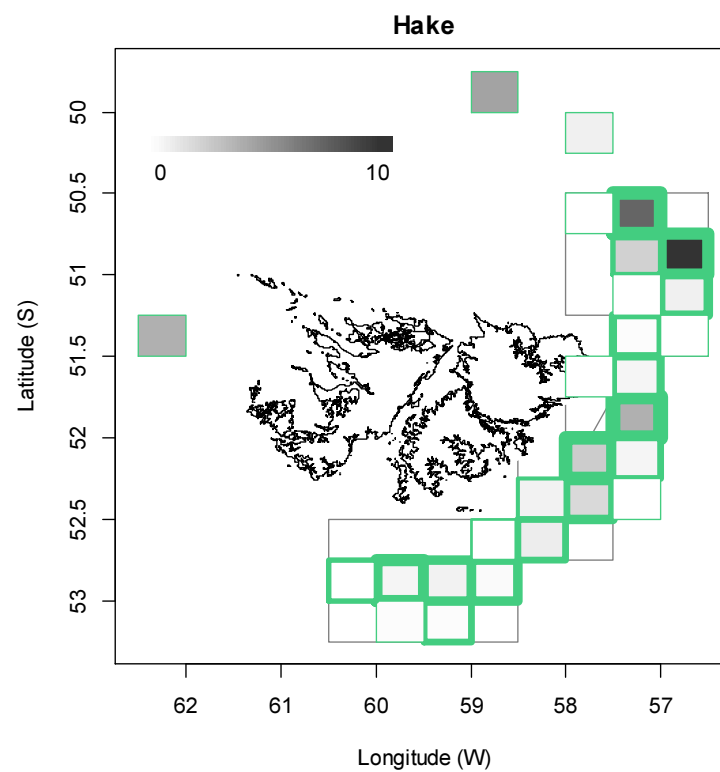
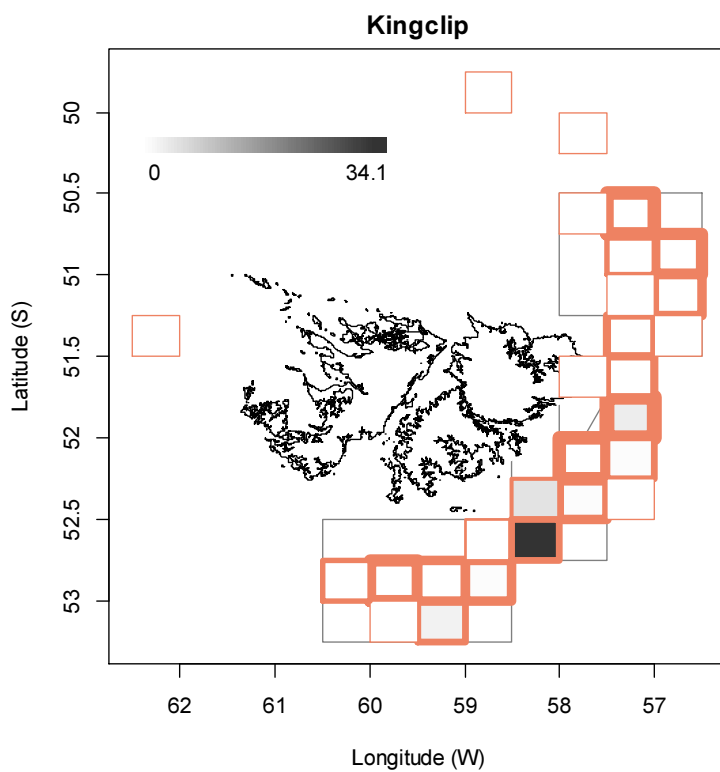
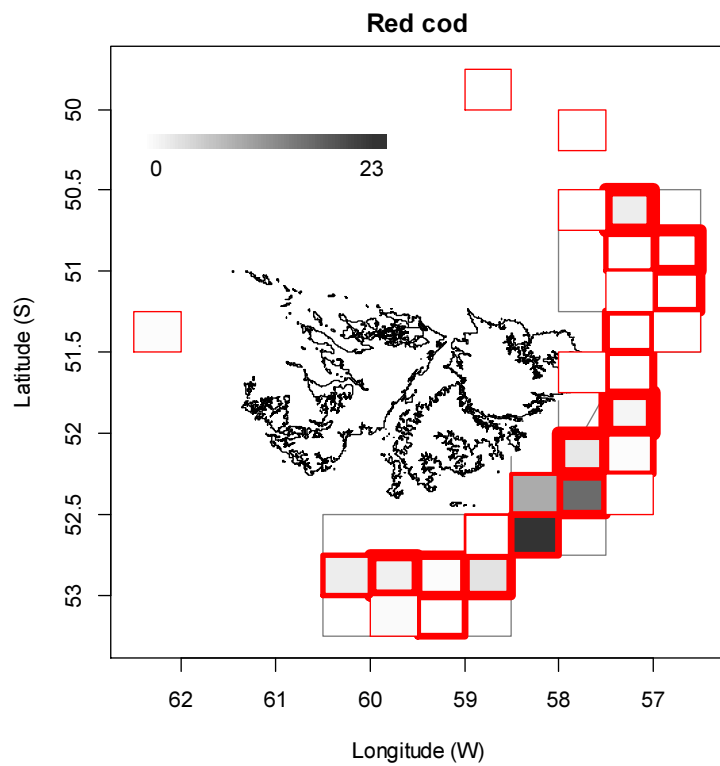
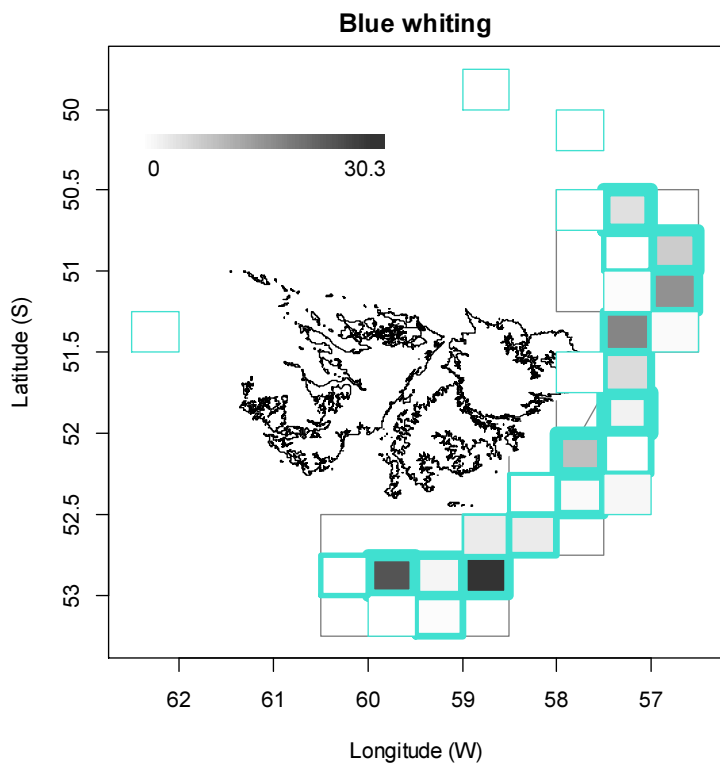
Table 3. Proportional (max. = 1) catch rates of calamari (LOL), numbers of vessels fishing (N), and average individual observer and commercial weights around the dates of exploratory fishing west of the Falkland Islands; compared to north and south in the Loligo Box.

Date	West				North				South			
	N	LOL	Wt. (kg)		N	LOL	Wt. (kg)		N	LOL	Wt. (kg)	
			(Obs)	(Com)			(Obs)	(Com)			(Obs)	(Com)
29/09	0	-	-	-	9.02	0.168	0.068	0.055	5.98	0.195	-	0.052
30/09	1	0.135	0.062	0.058	12.78	0.273	0.059	0.053	1.22	0.125	-	0.054
01/10	1	0.167	0.061	0.055	11	1.000	0.070	0.053	0	-	-	-
02/10	0	-	-	-	3	0.936	0.074	0.055	0	-	-	-

Bycatch

Of the 1004 calamari-target vessel-days in total (Table 1), only four vessel-days reported primary catches other than calamari, which were 66.6%, 59.9%, 54.0%, and 53.1% rock cod. In these four reports the rock cod catches ranged from 11.3 t to 21.2 t. The most common total bycatches reported for the Falkland calamari season were rock cod (1784 t, reported from 993 vessel-days), skates (Rajidae) (170 t, 585 vessel-days), blue whiting (*Micromesistius australis*) (130 t, 230 vessel-days), red cod (*Salilota australis*) (64 t, 217 vessel-days), kingclip (*Genypterus blacodes*) (46 t, 84 vessel-days), common hake (*Merluccius hubbsi*) (42 t, 347 vessel-days), Patagonian toothfish (*Dissostichus eleginoides*) (40 t, 347 vessel-days), and frogmouth (*Cottoperca gobio*) (19 t, 423 vessel-days). Relative distributions by grid of these bycatches are shown in Figure 11.





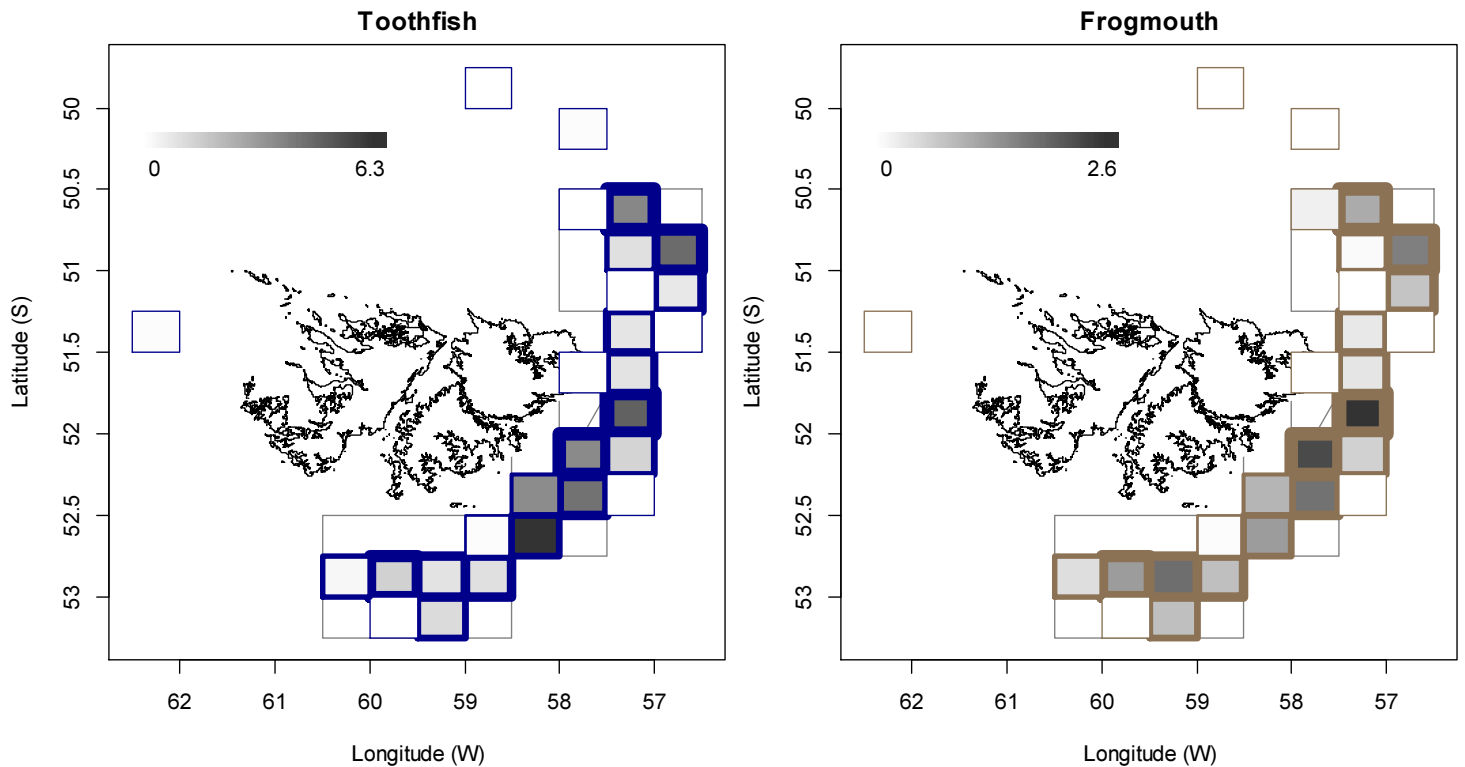


Figure 11. Distributions of the eight principal bycatches during 2nd calamari season 2016, by noon position grids. Thickness of grid lines is proportional to the number of vessel-days (1 to 121 per grid). Gray-scale is proportional to the bycatch biomass; maximum (tonnes) indicated on each plot.

References

- Agnew, D.J., Baranowski, R., Beddington, J.R., des Clers, S., Nolan, C.P. 1998. Approaches to assessing stocks of *Loligo gahi* around the Falkland Islands. *Fisheries Research* 35: 155-169.
- Agnew, D. J., Beddington, J. R., and Hill, S. 2002. The potential use of environmental information to manage squid stocks. *Canadian Journal of Fisheries and Aquatic Sciences*, 59: 1851–1857.
- Arkhipkin, A.I., Middleton, D.A.J. 2002. Sexual segregation in ontogenetic migrations by the squid *Loligo gahi* around the Falkland Islands. *Bulletin of Marine Science* 71: 109-127.
- Arkhipkin, A.I., Middleton, D.A.J., Barton, J. 2008. Management and conservation of a short-lived fishery resource: *Loligo gahi* around the Falkland Islands. *American Fisheries Society Symposium* 49: 1243-1252.
- Barton, J. 2002. Fisheries and fisheries management in Falkland Islands Conservation Zones. *Aquatic Conservation: Marine and Freshwater Ecosystems* 12: 127–135.
- Brooks, S.P., Gelman, A. 1998. General methods for monitoring convergence of iterative simulations. *Journal of computational and graphical statistics* 7:434-455.
- DeLury, D.B. 1947. On the estimation of biological populations. *Biometrics* 3: 145-167.
- Fisheries Committee. 2013. Re-allocation of fishing effort between 1st and 2nd *Loligo* seasons. Proposal to the Fisheries Committee, December 2013. 4 p.

- Gamerman, D., Lopes, H.F. 2006. Markov Chain Monte Carlo. Stochastic simulation for Bayesian inference. 2nd edition. Chapman & Hall/CRC.
- Grimmer, A. 2016a. Observer Report 1111. Technical Document, FIG Fisheries Department. 27 p.
- Grimmer, A. 2016b. Observer Report 1117. Technical Document, FIG Fisheries Department. 27 p.
- Iriarte, V. 2016. Observer Report 1112. Technical Document, FIG Fisheries Department. 24 p.
- Keningale, B. 2016. Observer Report 1115. Technical Document, FIG Fisheries Department. 36 p.
- Kuepfer, A. 2016. Observer Report 1116. Technical Document, FIG Fisheries Department. 30 p.
- Magnusson, A., Punt, A., Hilborn, R. 2013. Measuring uncertainty in fisheries stock assessment: the delta method, bootstrap, and MCMC. *Fish and Fisheries* 14: 325-342.
- Nash, J.C., Varadhan, R. 2011. optimx: A replacement and extension of the optim() function. R package version 2011-2.27. <http://CRAN.R-project.org/package=optimx>
- Patterson, K.R. 1988. Life history of Patagonian squid *Loligo gahi* and growth parameter estimates using least-squares fits to linear and von Bertalanffy models. *Marine Ecology Progress Series* 47: 65-74.
- Payá, I. 2010. Fishery Report. *Loligo gahi*, Second Season 2009. Fishery statistics, biological trends, stock assessment and risk analysis. Technical Document, Falkland Islands Fisheries Department. 54 p.
- Pierce, G.J., Guerra, A. 1994. Stock assessment methods used for cephalopod fisheries. *Fisheries Research* 21: 255 – 285.
- Punt, A.E., Hilborn, R. 1997. Fisheries stock assessment and decision analysis: the Bayesian approach. *Reviews in Fish Biology and Fisheries* 7:35-63.
- Roa-Ureta, R. 2012. Modelling in-season pulses of recruitment and hyperstability-hyperdepletion in the *Loligo gahi* fishery around the Falkland Islands with generalized depletion models. *ICES Journal of Marine Science* 69: 1403–1415.
- Roa-Ureta, R., Arkhipkin, A.I. 2007. Short-term stock assessment of *Loligo gahi* at the Falkland Islands: sequential use of stochastic biomass projection and stock depletion models. *ICES Journal of Marine Science* 64: 3-17.
- Rosenberg, A.A., Kirkwood, G.P., Crombie, J.A., Beddington, J.R. 1990. The assessment of stocks of annual squid species. *Fisheries Research* 8: 335-350.
- Shaw, P.W., Arkhipkin, A.I., Adcock, G.J., Burnett, W.J., Carvalho, G.R., Scherbich, J.N., Villegas, P.A. 2004. DNA markers indicate that distinct spawning cohorts and aggregations of Patagonian squid, *Loligo gahi*, do not represent genetically discrete subpopulations. *Marine Biology*, 144: 961-970.
- Winter, A. 2014. *Loligo* stock assessment, second season 2014. Technical Document, Falkland Islands Fisheries Department. 30 p.
- Winter, A. 2015. Falkland calamari stock assessment, second season 2015. Technical Document, Falkland Islands Fisheries Department. 25 p.

- Winter, A., Arkhipkin, A. 2015. Environmental impacts on recruitment migrations of Patagonian longfin squid (*Doryteuthis gahi*) in the Falkland Islands with reference to stock assessment. Fisheries Research 172: 85-95.
- Winter, A., Jones, J., Shcherbich, Z., Iriarte, V. 2016. Falkland calamari stock assessment survey, 2nd season 2016. Technical Document, Falkland Islands Fisheries Department. 22 p.
- Zhang, H.-M., Bates, J.J., Reynolds, R.W. 2006. Assessment of composite global sampling: Sea surface wind speed. Geophysical Research Letters 33: L17714.

Appendix

Falkland calamari individual weights

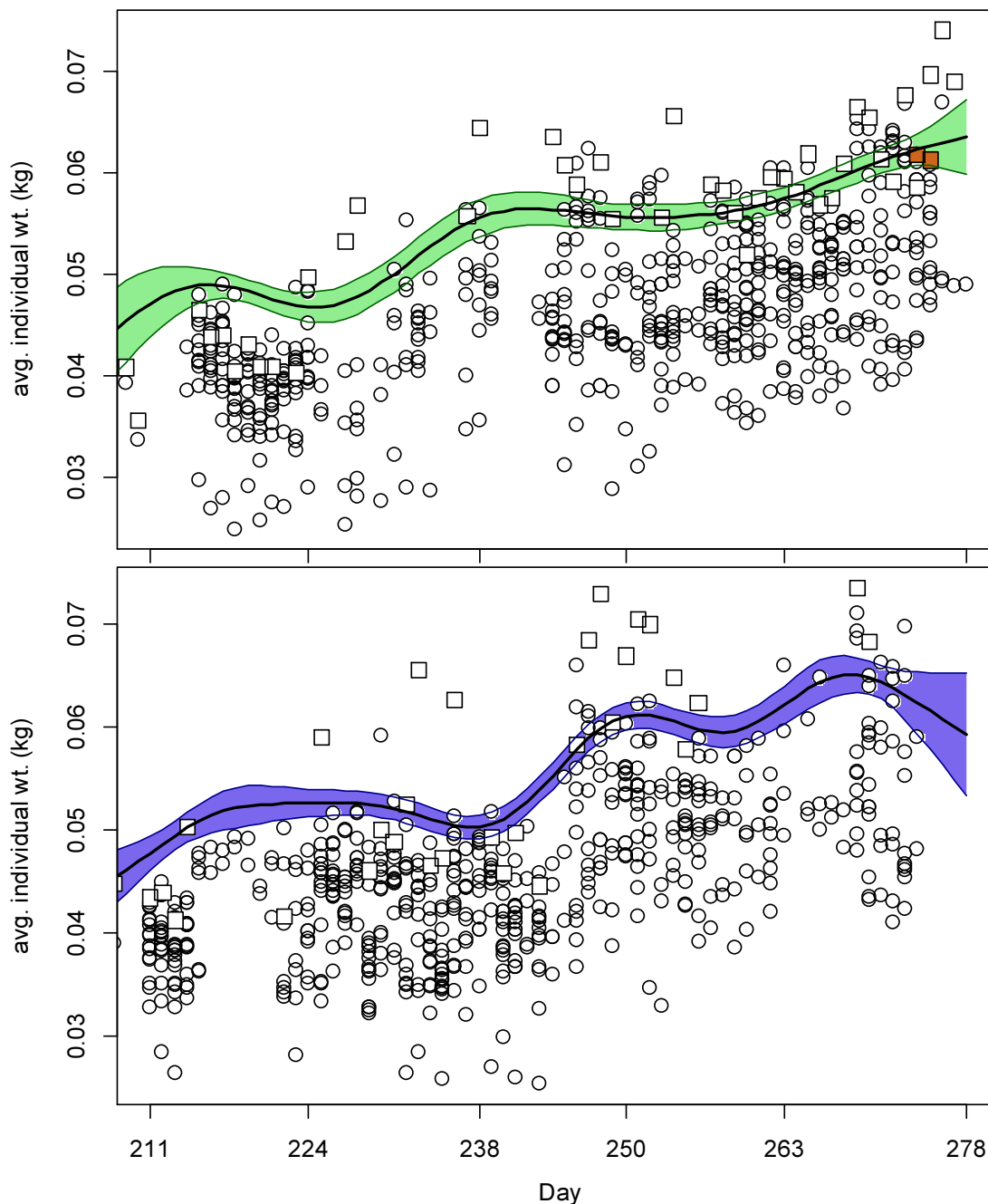


Figure A1. North (top) and south (bottom) sub-area daily average individual calamari weights from commercial size categories per vessel (circles) and observer measurements (squares). The two brown squares in the north plot are from the vessel fishing west of the Falkland Islands, and were not otherwise included in the weight trend calculations. GAMs of the daily trends \pm 95% confidence intervals (centre lines and colour under-shading).

To smooth fluctuations, generalized additive model (GAM) trends were calculated of daily average individual weights. North and south sub-areas were calculated separately. For continuity, the GAMs were calculated using all pre-season survey and in-season data

contiguously. North and south GAMs were first calculated separately on the commercial and observer data. The commercial data GAMs were taken as the baseline trends, and calibrated to the observer data GAMs in proportion to the correlation between the commercial data and observer data GAMs. For example, if the season average individual weight estimate from commercial data was 0.052 kg, the season average individual weight estimate from observer data was 0.060 kg, and the coefficient of determination (R^2) between commercial and observer GAM trends was 86%, then the resulting trend of daily average individual weights was calculated as the commercial data GAM values + $(0.060 - 0.052) \times 0.86$. This way, both the greater day-to-day consistency of the commercial data trends, and the greater point value accuracy of the observer data, are represented in the calculations. GAM plots of the north and south sub-areas are shown in Figure A1.

Prior estimates and CV

The pre-season survey (Winter et al., 2016) had estimated Falkland calamari biomasses of 15,844 t (standard deviation: $\pm 2,711$ t) north of 52° S and 27,736 t (standard deviation: 3,701 t) south of 52° S. From modelled survey catchability, Payá (2010) had estimated average net escapement of up to 22%, which was added to the standard deviation:

$$15,844 \pm \left(\frac{2,711}{15,844} + .22 \right) = 15,844 \pm 39.1\% = 15,844 \pm 6,196 \text{ t} \quad (\text{A1-N})$$

$$27,736 \pm \left(\frac{3,701}{27,736} + .22 \right) = 27,736 \pm 35.3\% = 27,736 \pm 9,803 \text{ t} \quad (\text{A1-S})$$

The 22% was added as a linear increase in the variability, but was not used to reduce the total estimate, because calamari that escape one trawl are likely to be part of the biomass concentration that is available to the next trawl.

Calamari numbers at the start of the season, day 211, were estimated as the survey biomasses divided by the GAM-predicted individual weight averages for the survey: 0.040 kg north, 0.045 kg south (Figure A1), and 0.042 combined. Average coefficients of variation (CV) of the GAM over the duration of the pre-season survey were 6.0% north and 4.2% south, and CV of the length-weight conversion relationship (equation 8) were 7.4% north and 6.3% south. Combining all sources of variation with the pre-season survey biomass estimates and average individual weight averages gave estimated calamari numbers at season start (July 29th; day 211) of:

$$\begin{aligned} \text{prior } N_{N \text{ day } 211} &= \frac{15,844 \times 1000}{0.040} \pm \sqrt{39.1\%^2 + 6.0\%^2 + 7.4\%^2} \\ &= 0.395 \times 10^9 \pm 40.3\% \end{aligned}$$

$$\begin{aligned} \text{prior } N_{S \text{ day } 211} &= \frac{27,736 \times 1000}{0.045} \pm \sqrt{35.3\%^2 + 4.2\%^2 + 6.3\%^2} \\ &= 0.618 \times 10^9 \pm 36.1\% \end{aligned}$$

Priors were normalized for the combined fishing zone average, to produce better continuity as vessels fish sometimes north and sometimes south:

$$\begin{aligned} \text{nprior } N_{N \text{ day } 211} &= \left(\frac{(15,844 + 27,736) \times 1000}{0.042} \right) \times \left(\frac{\text{prior } N_{N \text{ day } 211}}{\text{prior } N_{N \text{ day } 211} + \text{prior } N_{S \text{ day } 211}} \right) \\ &= 0.404 \times 10^9 \pm 40.3\% \end{aligned} \quad (\text{A2-N})$$

$$\begin{aligned} \text{nprior } N_{S \text{ day } 211} &= \left(\frac{(15,844 + 27,736) \times 1000}{0.042} \right) \times \left(\frac{\text{prior } N_{S \text{ day } 211}}{\text{prior } N_{N \text{ day } 211} + \text{prior } N_{S \text{ day } 211}} \right) \\ &= 0.632 \times 10^9 \pm 36.1\% \end{aligned} \quad (\text{A2-S})$$

The catchability coefficient (q) prior for the north sub-area was taken on day 214, when 2 vessels first fished north and the initial depletion period north started. The abundance prior (N) on day 214 was calculated as the survey abundance on start day 211 discounted for three days of natural mortality (given that no catch had been taken in those three days):

$$\text{nprior } N_{N \text{ day } 214} = \text{nprior } N_{N \text{ day } 211} \times e^{-M \cdot (214 - 211)} - \text{CNMD}_{\text{day } 214} = 0.388 \times 10^9 \quad (\text{A3-N})$$

$$\begin{aligned} \text{prior } q_N &= C(N)_{N \text{ day } 214} / (\text{nprior } N_{N \text{ day } 214} \times E_{N \text{ day } 214}) \\ &= (C(B)_{N \text{ day } 214} / \text{Wt}_{N \text{ day } 214}) / (\text{nprior } N_{N \text{ day } 214} \times E_{N \text{ day } 214}) \\ &= (155.3 \text{ t} / 0.049 \text{ kg}) / (0.388 \times 10^9 \times 2 \text{ vessel-days}) \\ &= 4.109 \times 10^{-3} \text{ vessels}^{-1} \text{ A} \end{aligned} \quad (\text{A4-N})$$

The catchability coefficient (q) prior for the south sub-area was taken on day 211, when all 15 vessels that had entered the fishery were operating south. As this was the first scheduled day of the season, no discount was applicable for either natural mortality or catch.

$$\begin{aligned} \text{prior } q_S &= C(N)_{S \text{ day } 211} / (\text{nprior } N_{S \text{ day } 211} \times E_{S \text{ day } 211}) \\ &= (C(B)_{S \text{ day } 211} / \text{Wt}_{S \text{ day } 211}) / (\text{nprior } N_{S \text{ day } 211} \times E_{S \text{ day } 211}) \\ &= (525.7 \text{ t} / 0.048 \text{ kg}) / (0.632 \times 10^9 \times 15 \text{ vessel-days}) \\ &= 1.161 \times 10^{-3} \text{ vessels}^{-1} \text{ B} \end{aligned} \quad (\text{A4-S})$$

CVs of the priors were calculated as the sums of variability in $\text{nprior } N$ (equations A2) plus variability in the catches of vessels on the start days (day 214 N and day 211 S):

$$\begin{aligned} \text{CV}_{\text{prior } N} &= \sqrt{40.3\%^2 + \left(\frac{\text{SD}(C(B)_{N \text{ vessels day } 214})}{\text{mean}(C(B)_{N \text{ vessels day } 214})} \right)^2} \\ &= \sqrt{40.3\%^2 + 3.3\%^2} = 40.4\% \end{aligned} \quad (\text{A5-N})$$

^A On Figure 6-left.

^B On Figure 8-left.

$$\begin{aligned}
CV_{\text{prior S}} &= \sqrt{36.1\%^2 + \left(\frac{SD(C(B)_{S \text{ vessels day 211}})}{\text{mean}(C(B)_{S \text{ vessels day 211}})} \right)^2} \\
&= \sqrt{36.1\%^2 + 27.7\%^2} = 45.5\% \quad \text{(A5-S)}
\end{aligned}$$

Depletion model estimates and CV

For the north sub-area, the equivalent of equation 2 with three N_{day} was optimized on the difference between predicted catches and actual catches (equation 3), resulting in parameters values:

$$\begin{aligned}
\text{depletion } N1_{N \text{ day 214}} &= 0.749 \times 10^9; & \text{depletion } N2_{N \text{ day 218}} &= 0.151 \times 10^3 \\
\text{depletion } N3_{N \text{ day 275}} &= 0.772 \times 10^9 \\
\text{depletion } Q_N &= 0.880 \times 10^{-3} C \quad \text{(A6-N)}
\end{aligned}$$

The root-mean-square deviation of predicted vs. actual catches was calculated as the CV of the model:

$$\begin{aligned}
CV_{\text{rmsd N}} &= \frac{\sqrt{\sum_{i=1}^n (\text{predicted } C(N)_{N \text{ day } i} - \text{actual } C(N)_{N \text{ day } i})^2 / n}}{\text{mean}(\text{actual } C(N)_{N \text{ day } i})} \\
&= 1.360 \times 10^6 / 3.719 \times 10^6 = 36.6\% \quad \text{(A7-N)}
\end{aligned}$$

$CV_{\text{rmsd N}}$ was added to the variability of the GAM-predicted individual weight averages for the season (Figure A1-N); equal to a CV of 1.7% north. CVs of the depletion were then calculated as the sum:

$$\begin{aligned}
CV_{\text{depletion N}} &= \sqrt{CV_{\text{rmsd N}}^2 + CV_{\text{GAM Wt N}}^2} = \sqrt{36.6\%^2 + 1.7\%^2} \\
&= 36.6\% \quad \text{(A8-N)}
\end{aligned}$$

For the south sub-area, the equivalent of equation 2 with two N_{day} was optimized on the difference between predicted catches and actual catches (equation 3), resulting in parameters values:

$$\begin{aligned}
\text{depletion } N1_{S \text{ day 211}} &= 1.073 \times 10^9; & \text{depletion } N2_{S \text{ day 230}} &= 2.535 \times 10^1 \\
\text{depletion } Q_S &= 0.649 \times 10^{-3} D \quad \text{(A6-S)}
\end{aligned}$$

The normalized root-mean-square deviation of predicted vs. actual catches was calculated as the CV of the model:

^C On Figure 6-left.

^D On Figure 8-left.

$$\begin{aligned}
CV_{\text{rmsd S}} &= \frac{\sqrt{\sum_{i=1}^n (\text{predicted } C(N)_{\text{S day } i} - \text{actual } C(N)_{\text{S day } i})^2 / n}}{\text{mean}(\text{actual } C(N)_{\text{S day } i})} \\
&= 1.235 \times 10^6 / 3.432 \times 10^6 = 36.0\% \quad (\text{A7-S})
\end{aligned}$$

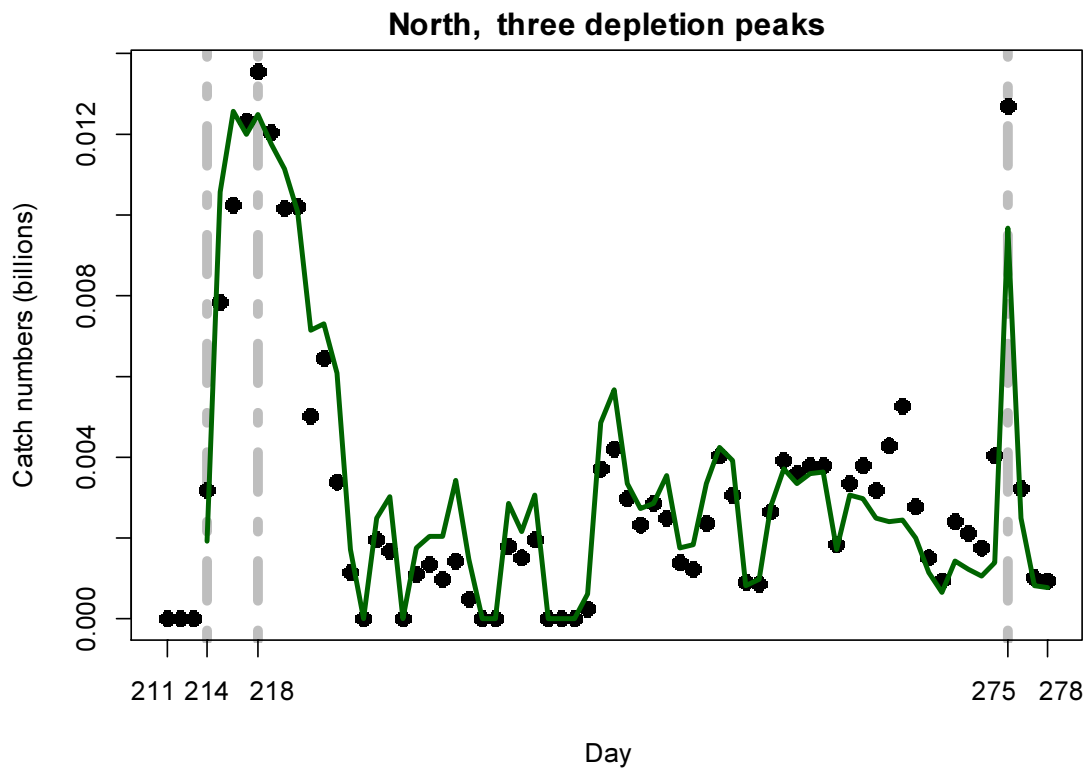
$CV_{\text{rmsd S}}$ was added to the variability of the GAM-predicted individual weight averages for the season (Figure A1-S); equal to a CV of 1.4% south. CVs of the depletion were then calculated as the sum:

$$\begin{aligned}
CV_{\text{depletion S}} &= \sqrt{CV_{\text{rmsd S}}^2 + CV_{\text{GAM WtS}}^2} = \sqrt{36.0\%^2 + 1.4\%^2} \\
&= 36.0\% \quad (\text{A8-S})
\end{aligned}$$

Combined Bayesian models

For the north sub-area, the joint optimization of equations 3 and 4 resulted in parameters values:

$$\begin{aligned}
\text{Bayesian } N1_{\text{N day } 214} &= 0.330 \times 10^9; & \text{Bayesian } N2_{\text{N day } 218} &= 0.028 \times 10^9 \\
\text{Bayesian } N3_{\text{N day } 275} &= 0.270 \times 10^9 \\
\text{Bayesian } q_N &= 2.916 \times 10^{-3} \text{ E} \quad (\text{A9-N})
\end{aligned}$$



^E On Figure 6-left.

Figure A2-N [previous page]. Daily catch numbers estimated from actual catch (black points) and predicted from the depletion model (green line) in the north sub-area.

These parameters produced the fit between predicted and actual catches shown in Figure A2-N. The period of non-depletion between day 258 and the peak on day 275 (Figure 4) resulted in consistent under-prediction over that portion of the time series.

For the south sub-area, the joint optimization of equations 3 and 4 resulted in parameters values:

$$\begin{aligned}
 \text{Bayesian } N1_S \text{ day 211} &= 0.647 \times 10^9; & \text{Bayesian } N2_S \text{ day 230} &= 0.057 \times 10^9 \\
 \text{Bayesian } q_S &= 1.120 \times 10^{-3} \text{ }^F & &
 \end{aligned}
 \tag{A9-S}$$

These parameters produced the fit between predicted and actual catches shown in Figure A2-S.

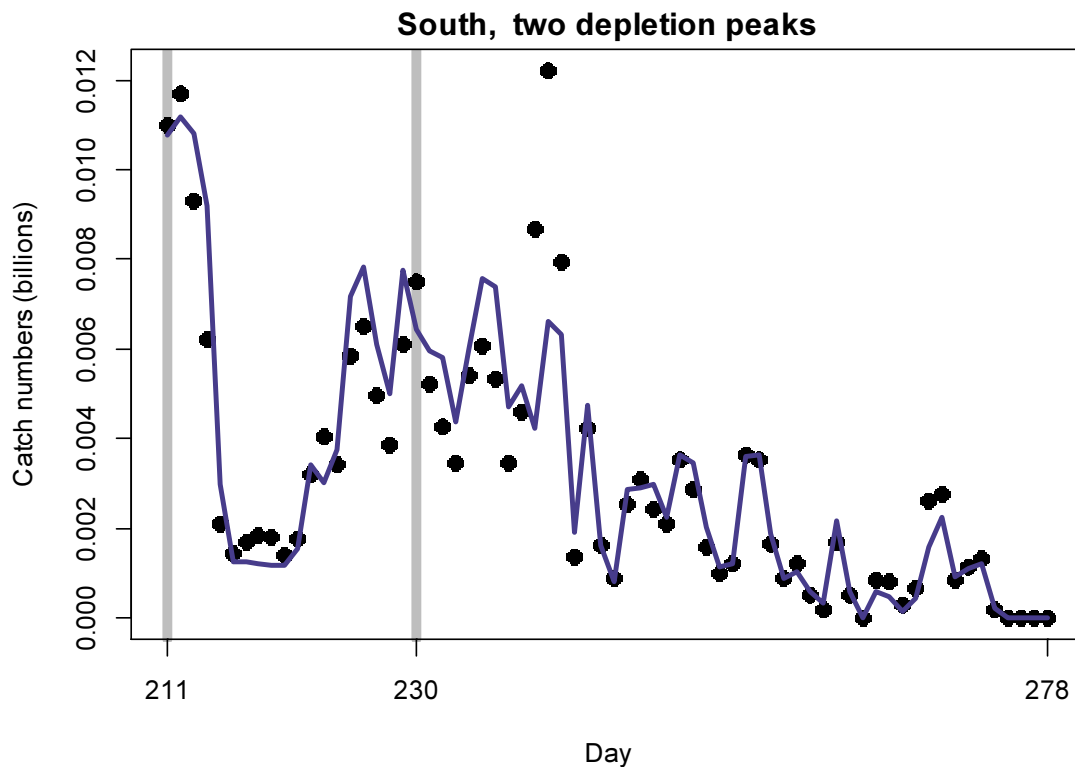


Figure A2-S. Daily catch numbers estimated from actual catch (black points) and predicted from the depletion model (blue line) in the south sub-area.

^F On Figure 8-left.